Elevated Hydrostatic Pressure Triggers Mitochondrial Fission and Decreases Cellular ATP in Differentiated RGC-5 Cells

Won-Kyu Ju,[1] Quan Liu,[1] Keun-Young Kim,[2] Jonathan G. Crowston,[1] James D. Lindsey,[1] Neeraj Agarwal,[3] Mark H. Ellisman,[2] Guy A. Perkins,[2] and Robert N. Weinreb[1]

Purpose. Mitochondrial fission is a cellular response to stress that has an important role in neuronal cell death in neurodegenerative diseases. The purpose of this study was to determine whether elevated hydrostatic pressure induces mitochondrial fission and dysfunction in cultured retinal ganglion cells.

Methods. RGC-5 cells were differentiated with succinyl concanavalin A (50 μg/mL) and transferred to a pressurized incubator in which 30 mm Hg of pressure was applied for 1, 2, or 3 days. As a control, differentiated cells from an identical passage were incubated simultaneously in a conventional incubator at each of the time points. Live RGC-5 cells were then labeled with a red fluorescent mitochondrial dye and mitochondrial morphology was assessed by fluorescence microscopy and electron microscopy. After elevated hydrostatic pressure, the cellular adenosine triphosphate (ATP) levels were also measured by a luciferase-based assay.

Results. Mitochondrial fission, characterized by the conversion of tubular fused mitochondria into isolated small organelles, was triggered in $>74.3\% \pm 1.9\%$ of mitochondria at 3 days after elevated hydrostatic pressure. Only $4.7\% \pm 1.4\%$ of nonpressurized control cells displayed mitochondrial fission after 3 days. Electron microscopy showed that elevated hydrostatic pressure for 3 days induced abnormal cristae depletion and decreased the length of the mitochondria. On elevation of hydrostatic pressure, the fission-linked protein, Drp-1 was translocated from the cytosol to the mitochondria. Elevated hydrostatic pressure also resulted in a significant, time-dependent reduction of cellular ATP.

Conclusions. Elevated hydrostatic pressure triggered mitochondrial fission, abnormal cristae depletion, Drp-1 translocation, and cellular ATP reduction in differentiated RGC-5 cells. Increased understanding of the molecular mechanisms that regulate the cellular response to elevated pressure including mitochondrial fission may provide new therapeutic targets for protecting RGCs from elevated hydrostatic pressure. (*Invest Ophthalmol Vis Sci.* 2007;48:2145–2151) DOI:10.1167/iovs.06-0573

Elevated intraocular pressure (IOP) is an important risk factor for optic nerve damage in glaucoma.[1] The impairment of retrograde axonal transport of neurotrophins and secondary insults induced by elevated IOP have been proposed as mechanisms that contribute to retinal ganglion cell (RGC) death in glaucoma.[2,3] However, the precise pathophysiological mechanism that leads to RGC death in glaucomatous optic nerve damage by elevated IOP remains unknown. Mitochondrial changes have been involved in the pathophysiology of neuronal death and it is reasonable to speculate that they, too, may cause glaucomatous optic neuropathy.

Mitochondria are the cellular organelles that generate adenosine triphosphate (ATP). In addition, they are the central players in initiating cell death by apoptosis.[4,5] In healthy cells, mitochondria are autonomous and morphologically dynamic organelles that structurally reflect a precise balance of ongoing fission and fusion within a cell.[6–9] This balance is regulated by a family of dynamin-related GTPases that exert opposing effects. OPA1 and the mitofusins are necessary for mitochondria fusion, whereas Drp-1 regulates mitochondrial fission.[6] Recent studies have indicated that mitochondrial fission occurs before and during apoptosis, resulting in small, round, and more numerous organelles.[10–14] Moreover, mitochondrial dysfunction has been identified in a wide variety of neurodegenerative diseases including aging and cancer.[15–22] Although evidence of abnormal mitochondrial respiration has been reported in patients with glaucoma[23] and mitochondria have been shown to play a role in RGC apoptosis in experimental rodent models of glaucoma,[22] it is not known whether mitochondrial dysfunction per se is present in glaucoma. We hypothesized that elevated IOP, a major risk factor for glaucoma, induces mitochondrial dysfunction in RGCs.

To investigate mitochondrial dysfunction in RGC, we investigated structural and functional changes of mitochondria in RGC death induced by elevated hydrostatic pressure.

Materials and Methods

Culture of RGC-5 Cells

The rat retinal ganglion cell line, RGC-5, transformed with adenovirus carrying E1A was cultured in Dulbecco's modified Eagle's medium (DMEM) containing 10% fetal calf serum (FCS), 100 U/mL penicillin and 100 μg/mL streptomycin (Sigma-Aldrich, St. Louis, MO) in 5% CO_2 at 37°C.[24]

Differentiation of RGC-5 Cells

Differentiation of RGC-5 cells was performed as previously described.[24] Nondifferentiated cells were first seeded in the 100-mm tissue culture dishes at a density of 5×10^4. After 4 hours, when the cells attached to the dish, the dishes were rinsed with serum-free

From the [1]Hamilton Glaucoma Center and Department of Ophthalmology, University of California San Diego, La Jolla, California; the [2]National Center for Microscopy and Imaging Research, School of Medicine, University of California, San Diego, La Jolla, California; and the [3]Department of Cell Biology and Genetics, University of North Texas Health Science Center, Fort Worth, Texas.

Supported by National Eye Institute Grants EY01466 (JDL) and EY105990 (RNW) and National Center for Research Resources Grant P41 RR004050 (MHE).

Submitted for publication May 26, 2006; revised October 31, 2006, and January 2, 2007; accepted March 8, 2007.

Disclosure: **W.-K. Ju**, None; **Q. Liu**, None; **K.-Y. Kim**, None; **J.G. Crowston**, None; **J.D. Lindsey**, None; **N. Agarwal**, None; **M.H. Ellisman**, None; **G.A. Perkins**, None; **R.N. Weinreb**, None

The publication costs of this article were defrayed in part by page charge payment. This article must therefore be marked "*advertisement*" in accordance with 18 U.S.C. §1734 solely to indicate this fact.

Corresponding author: Won-Kyu Ju, Hamilton Glaucoma Center, University of California San Diego, La Jolla, CA 92037; danielju@glaucoma.ucsd.edu.

medium three to five times. The dishes were then incubated with DMEM without FCS for 24 hours under the conditions just described. The medium was then changed to DMEM containing 10% FCS and supplemented with succinyl concanavalin A (sConA; 50 μg/mL; Sigma-Aldrich), a nontoxic derivative of the lectin concanavalin A.[24,25] Three days after treatment with sConA, the cells were exposed to elevated hydrostatic pressure up to 3 days.

Pressure System

A pressurized incubator was designed to expose the cells to elevated hydrostatic pressure.[26–29] The Plexiglas pressure chamber was connected via a low-pressure two-stage regulator (Gilmont Instruments; Barnant Co., Barrington, IL) to a certified source of 5% CO_2/95% air (Airgas Inc., San Diego, CA). This arrangement provided constant hydrostatic pressure within ±1 mm Hg and ranging from 0 to 200 mm Hg. Gas to the chamber was warmed and humidified by bubbling through two liters of water. Both the water flask and the pressure chamber were maintained at 37°C by placing them inside an electronically controlled conventional incubator. Gas flow of 70 mL/min was monitored by using a ball-type flow gauge regulated with a needle valve in the outlet circuit. Pressure was monitored using a diaphragm-driven dial pressure gauge plumbed into the inlet circuit adjacent to the pressure chamber inlet. This pressure gauge was readable through a double-paned window present in the door of the incubator chamber. The key strengths of our device are that gas flow and pressure can be easily and accurately regulated to ±1 mm Hg by using the flowmeter and the low-pressure, two-stage regulator.

The possibility that elevated hydrostatic pressure could alter gas exchange was assessed by analyzing blood gassed in culture medium in pressure and control cultures before and after 1, 2, or 3 days of pressurization. Measurements for pH, pCO_2 and pO_2 analysis were performed with a portable blood gas analyzer (iSTAT Corp. East Windsor, NJ). Briefly, the 100-mm culture dishes were removed from the incubator and 100 μL of culture medium was transferred by micropipette to the detection chip within 2 seconds. The cap on the chip was then immediately sealed, and the chip was directly inserted into the analyzer.

To examine the time course of cellular responses, elevated hydrostatic pressure was maintained for 1, 2, or 3 days. Control differentiated cells plated from an identical passage of RGC-5 cells were incubated simultaneously in a conventional 5% CO_2 culture incubator at 37°C.

Morphology Analysis for Mitochondria

After application of elevated hydrostatic pressure, mitochondria in the RGC-5 cells were labeled by the addition of a red fluorescent mitochondrial dye to the cultures (100 nM final concentration; MitoTracker Red CMXRos; Invitrogen-Molecular Probes, Eugene, OR) and maintaining it for 20 minutes in a CO_2 incubator. This dye is concentrated in active mitochondria by a process that is dependent on mitochondrial membrane potential (i.e., accumulation is inhibited by actinomycin A but not by rotenone). Previous double labeling studies with this dye and antibodies to the mitochondrial protein cytochrome *c* oxidase showed that it specifically labels mitochondria.[30] The cultures were subsequently fixed with 0.5% glutaraldehyde (Ted Pella, Redding, CA) in Dulbecco's phosphate-buffered saline (DPBS) for 30 minutes at 4°C and counterstained with Hoechst 33342 (1 μg/mL; Invitrogen-Molecular Probes) in DPBS. Mitochondrial morphology was observed by fluorescence microscopy.

Images were captured by fluorescence microscopy (Eclipse E800; Nikon Instruments Inc., Melville, NY) equipped with a digital camera (SPOT; Diagnostic Instrument, Sterling Heights, MI). Images were acquired using emission filters of 457, or 528, or 617 nm, collected by image-analysis software (Simple PCI, ver. 6.0; Compix Inc., Cranberry Township, PA), and exported into image-management software (Photoshop; Adobe Systems, San Jose, CA).

The percentage of RGC-5 cells with fragmented mitochondria was scored with 600 cells per condition by two investigators in a masked fashion, and the scores were averaged. Data represent the mean ± SD of results in three independent experiments. The depth of focus using the 60× oil immersion lens was sufficient to distinguish swollen or round mitochondria from mitochondria undergoing mitochondrial fission.

Electron Microscopy

RGC-5 cells were grown on 35-mm glass-bottomed culture dishes (MatTek, Ashland, MA). After exposure of elevated hydrostatic pressure, cultures were fixed with a 37°C solution of 2% paraformaldehyde (Sigma-Aldrich) and 2.5% glutaraldehyde (Ted Pella) in 0.1 M sodium cacodylate (pH 7.4; Sigma-Aldrich), maintained at room temperature for 5 minutes, and then incubated for an additional 30 minutes on ice. Fixed cultures were then rinsed three times for 3 minutes each with 0.1 M sodium cacodylate plus 3 mM calcium chloride (Sigma-Aldrich, pH 7.4) on ice and then postfixed with 1% osmium tetroxide, 0.8% potassium ferrocyanide (Sigma-Aldrich), 3 mM calcium chloride in 0.1 M sodium cacodylate (pH 7.4) for 60 minutes and then washed three times for 3 minutes with ice-cold distilled water. Cultures were finally stained overnight with 2% uranyl acetate at 4°C, dehydrated in graded ethanol baths, and embedded in resin (Durcupan; Fluka, Buchs, Switzerland). Ultrathin (70 nm) sections were poststained with uranyl acetate and lead salts and evaluated by transmission electron microscope (1200FX; JEOL, Tokyo, Japan) operated at 80 kV. All reagents were purchased from Ted Pella, Inc., unless otherwise indicated. Images were recorded on film at 8000× magnification. The negatives were digitized at 1800 dpi (Cool scan system; Nikon), giving an image size of 4033 × 6010 pixels and a pixel resolution of 1.77 nm. For comparison of mitochondrial length, electron micrographs of thin sections were evaluated, as described previously.[31]

Western Blot Analysis

The cytosolic and mitochondrial fractions were isolated from cultured RGC-5 cells by differential centrifugation (Mitochondrial Isolation Kit; Pierce, Rockford, IL, used according to the manufacturer's Dounce homogenizer procedure). For Western blot analysis, mitochondria were lysed with 2% CHAPS (3-[3-cholamidopropyl]dimethylammonio-2-hydroxy-1-propanesulfonate) in TBS for protein analysis with a DC protein assay (Bio-Rad, Hercules, CA). The cytosolic or mitochondrial fractions were mixed with SDS-PAGE sample buffer and boiled for 10 minutes. Equivalent amounts of protein (10 μg) for each sample were loaded onto 4% to 12% precast polyacrylamide gradient gels (Invitrogen). The proteins were electrotransferred to a nitrocellulose membrane in Tris-glycine-methanol transfer buffer. The membrane was blocked for 1 hour at room temperature in PBS containing 5% nonfat dry milk and 0.05% Tween-20 and then incubated for 15 hours at 4°C with primary antibodies: polyclonal rabbit anti-human Drp1 (dynamin-related protein-1) antibody (H-300, cat. no. sc-32898, 1:1000; Santa Cruz Biotechnology Inc., Santa Cruz, CA), monoclonal mouse anti-actin antibody (Ab-1, cat. no. CP01, 1:10,000; Calbiochem, La Jolla, CA) and polyclonal rabbit anti-VDAC (Porin) antibody (Ab-5, cat. no. PC548T, 1:1000, Calbiochem). The actin or VDAC antibodies were used to confirm similar cytosol or mitochondrial protein loading in each lane to the Western blot analysis for Drp-1, respectively. The membrane was then rinsed with 0.05% Tween-20 in PBS and incubated for 2 hours at room temperature with peroxidase-conjugated goat anti-rabbit IgG for Drp-1 and VDAC antibodies (1:2000; Bio-Rad) or goat anti-mouse IgM for actin antibody (1:2000; Calbiochem). The blots were developed with a chemiluminescence detection kit (ECL Plus; GE Healthcare Bio-Sciences, Piscataway, NJ), used according to the manufacturer's recommendations. Images were analyzed by using a digital fluorescence imager (Storm 860; GE Healthcare Bio-Sciences). Band densities on the Western blot analysis were determined by computer (ImageQuant TL Analysis software; GE Healthcare Bio-Sciences).

Cellular ATP Measurement

The level of cellular ATP in RGC-5 cells was determined with a luciferase-based assay (CellTiter-Glo; Promega Corp., Madison, WI), accord-

ing to the manufacturer's recommendations. After the plates were developed, luminescence was measured in a microplate luminometer (Luminoskan; Labsystems, Helsinki, Finland). Each set of data was collected from multiple replicate wells of each experimental group ($n = 24$).[31,32] The total number of cells in parallel plates was estimated with an MTT assay or trypan blue assay. Results were normalized according to cell number.

Cell Viability Measurement

MTT Assay. Cell viability was measured in RGC-5 cells cultured in 96-well plates using 3-[4,5-dimethylthiazol-2yl]-2,5-diphenyl tetrazolium bromide (MTT) according to the manufacturer's recommendations (Cell Proliferation Kit 1; Roche Diagnostics, Indianapolis, IN). Briefly, cells are grown in 96-well plates with a final volume of 100-μL culture medium per well. At 3 days after exposure with elevated hydrostatic pressure, 10 μL of the MTT labeling reagent (final concentration 0.5 mg/mL) was added to each well, and the cultures were incubated in the conventional CO_2 incubator at 37°C for 4 hours. Next, 100 μL of the solubilization solution was added to each well, and the plates were incubated for 16 hours in a humidified atmosphere of a 5% CO_2 incubator at 37°C. Absorbance at 560 nm was then measured with a microplate reader (Spectra MAX; Molecular Devices Corp., Sunnyvale, CA). Data are presented as the percentage of cell viability in same-day control wells. Each set of data was collected from multiple replicate wells of each experimental group ($n = 24$).

Trypan Blue Assay. Cells on 96-well plates were briefly washed with 0.1 mL DPBS and treated with 50 μL of ATV (Invitrogen, Carlsbad, CA) for 5 minutes at 37°C. When all the cells were released, 0.1 mL of culture medium was added. A single-cell suspension was obtained by gentle trituration through a flame-polished Pasteur pipet and transferred to a separate tube. The total number of cells in each well was counted with a hemocytometer. Cell viability was determined by adding 20 μL of filtered 0.4% trypan blue PBS solution (Sigma-Aldrich) to 20 μL of the cell suspension, and 10 μL was loaded into a hemocytometer. Data are presented as the percentage of viable cells in control wells. Each set of data was collected from multiple replicate wells of each experimental group ($n = 5$).

Statistical Analysis

Experiments presented were repeated at least three times with triplicate samples. The data are presented as the mean ± SD. Comparison of two experimental conditions was evaluated using the unpaired Student's *t*-test. Comparison of three experimental conditions was evaluated using one-way ANOVA and the Bonferroni *t*-test. $P < 0.05$ was considered to be statistically significant.

Results

Effect of Hydrostatic Pressure in Culture Media

Gas analysis of samples of culture media 3 days after exposure to hydrostatic pressure found no significant difference in pH, pCO_2, or pO_2 between the pressure and control RGC-5 cultures (Table 1, $P > 0.5$, $n = 3$).

Effect of Elevated Hydrostatic Pressure on Mitochondrial Morphology

Mitochondria in control cells at 3 days showed a typical filamentous and fused mitochondrial network (Fig. 1A). At 1 and 2 days after elevated hydrostatic pressure, no morphologic changes were evident (i.e., mitochondria retained a filamentous mitochondrial network similar to that observed in nonpressurized control cells at each time point; data not shown). However, mitochondrial fission, characterized by the conversion of tubular fused mitochondria into isolated small organelles, was induced in 74.3% ± 1.9% of the cells at 3 days after elevated hydrostatic pressure (Fig. 1B; $n = 5$ cultures, $P < 0.05$). In contrast, only 4.7% ± 1.4% of control RGC-5 cells displayed mitochondrial fission at 3 days (Fig. 1B). Elevated hydrostatic pressure did not induce mitochondrial fission in undifferentiated RGC-5 cells (data not shown). Transmission electron microscopy showed that nonpressurized control cells contained a classic long tubular form of mitochondria with abundant cristae (Fig. 2A). In contrast, elevated hydrostatic pressure results in circular vesicle form of mitochondria with abnormal cristae depletion (Fig. 2B). As shown in Figure 2C, the mean length of mitochondrial cross section was significantly decreased (from 845.0 ± 41.0 nm in control cultures to 571.3 ± 22.7 nm) in cells exposed to elevated hydrostatic pressure ($P < 0.001$ by *t*-test, $n = 222$ for control cells and 217 for pressure-treated cells).

Effect of Elevated Hydrostatic Pressure on Drp-1 Translocation

To assess whether the pressure-induced mitochondrial fission was associated with Drp-1 translocation, we examined the relative amounts of Drp-1 within cell fractions from the cytosol and mitochondria. As shown in Figure 3A, Drp-1 in the control cells was primarily within the cytosolic fraction. This result agrees with those in prior studies showing that Drp-1 resides in the cytoplasm of healthy cells.[8,10,11] Pressure treatment decreased Drp-1 by 55.6% ± 2.2% in the cytosolic fraction, compared to the control ($n = 3$, Fig. 3B). In contrast, Drp-1 was increased by 57.4% ± 8.7% in mitochondrial fraction at 3 days after elevated hydrostatic pressure. This indicates that elevated hydrostatic pressure induces Drp-1 translocation from the cytosol to mitochondria.

Effect of Elevated Hydrostatic Pressure on Cellular ATP

Exposure of RGC-5 cells to elevated hydrostatic pressure induced a significant, time-dependent reduction in cellular ATP level (42.6% ± 3%; $n = 24$ replicate wells, Fig. 4). According to the MTT assay, cell survival at 3 days after elevated hydrostatic pressure was 75.5% ± 9% relative to cell survival in the control cultures ($n = 24$ replicate wells, Fig. 5A). In addition, we counted the absolute number of viable cells, to measure non–mitochondria-based cell viability at 3 days after elevated hydrostatic pressure. Trypan blue staining showed that cell survival

Table 1. Measurement of pH, pCO_2, and pO_2 after 3 Days with or without Pressure Application

Treatment	Control (No Cells)	Control (with Cells)	Pressure (with Cells)
Time (days)	3	3	3
pH	7.82 ± 0.01	7.62 ± 0.05	7.66 ± 0.09
pCO_2 (mm Hg)	24.3 ± 0.7	24.8 ± 2.3	25.5 ± 4.5
pO_2 (mm Hg)	132.6 ± 5.85	122 ± 3.6	125 ± 6.0

Statistical analysis (Student's unpaired *t*-test) showed no significant difference in pH, pCO_2, or pO_2 between the pressure and control RGC-5 culture media ($P > 0.5$, $n = 3$).

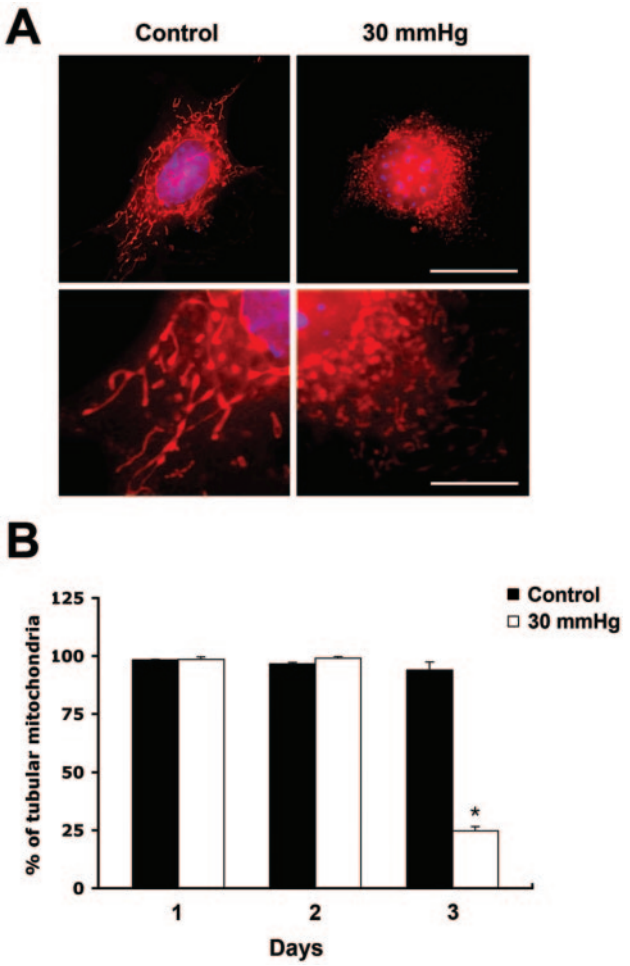

FIGURE 1. Mitochondrial fission after exposure to elevated hydrostatic pressure. Differentiated RGC-5 cells were exposed to elevated hydrostatic pressure (30 mm Hg) for 3 days. (**A**) Mitochondrial red staining. Higher magnification shows that mitochondrial fission, which is characterized by the conversion of tubular fused mitochondria into isolated small organelles, was triggered at 3 days after elevated hydrostatic pressure. (**B**) Differentiated RGC-5 cells were treated with elevated hydrostatic pressure (30 mm Hg) for 1, 2, or 3 days. The percentage of cells with fragmented mitochondria was determined after staining with the mitochondrial dye. *Significant at $P < 0.05$ compared with nonpressurized cells at 3 days. Data represent the mean ± SD of results in three independent experiments, with 600 cells analyzed per condition. Scale bar: (*top*) 20 μm; (*bottom*) 10 μm.

after 3 days was 85.3% ± 3% in the control cultures and 69.0% ± 3% in the cultures exposed to elevated hydrostatic pressure (Fig. 5B; $n = 5$). Thus, survival in the pressure-treated cultures was 81% (69.0/85.3) of the survival in the control cultures. There was no significant difference between the cell death measurements obtained using MTT or trypan blue.

DISCUSSION

These data demonstrate that elevated hydrostatic pressure triggers mitochondrial fission, cristae depletion, Drp-1 translocation from the cytosol to mitochondria, and cellular ATP reduction in sConA-differentiated RGC-5 cells. These results indicate that elevated hydrostatic pressure can induce mitochondrial structural changes and bioenergetic impairment.

Emerging evidence indicates that mitochondrial morphology and dynamics play an important role in cell and animal physiology. An imbalance in the control of mitochondrial fusion and fission dramatically alters overall mitochondrial morphology.[6,7] In addition, recent evidence suggests that the mitochondrial fission machinery actively participates in the process of apoptosis and that excessive mitochondrial fission leads to breakdown of the mitochondrial network, loss of mitochondrial DNA, respiratory defects and an increase in reactive oxygen species in mammalian cells.[6,10,11,33–35] In the present study, elevated hydrostatic pressure caused breakdown of the mitochondrial network by mitochondrial fission. Electron microscopy confirmed this mitochondrial fission transforms the normally elongated mitochondria to the circular vesicle form of mitochondria. In addition, it revealed that pressure treatment induces abnormal cristae depletion and decreased length of mitochondria. Indirect evidence suggests that mitochondria with depleted cristae may cause bioenergetic impairment.[31,36–38] It has also been reported that increased mitochondrial fission is accompanied by cytochrome *c* release and is upstream of caspase activation during apoptosis.[39] Thus, we propose that mitochondrial fission may be a marker for upstream signaling events that contribute to RGC degeneration induced by elevated hydrostatic pressure.

Recent evidence has indicated that mitochondrial fission is associated with the translocation of Drp-1 from cytoplasm to defined spots on the mitochondrial membrane.[12,13,40] Consistent with these prior studies, we found that Drp-1 protein was decreased in the cytosolic fraction in the pressure-treated cells but was increased in the mitochondrial fraction. This indicates that Drp-1 translocation in our model contributes to the mechanism of mitochondrial fission in differentiated RGC-5 cells

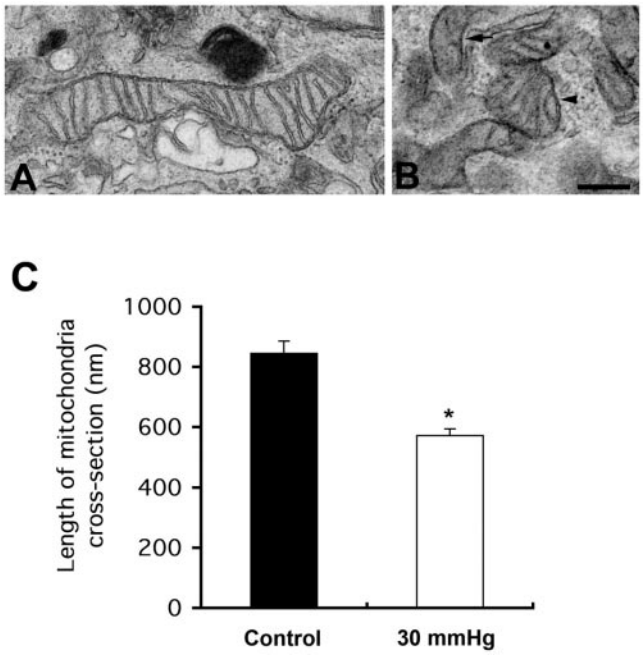

FIGURE 2. Abnormal cristae structure after exposure to elevated hydrostatic pressure. Differentiated RGC-5 cells were exposed to elevated hydrostatic pressure (30 mm Hg) for 3 days. Electron micrographs of a thin section of RGC-5 cells show the classic long tubular form of mitochondria, with closely spaced cristae in nonpressurized control cells (**A**), whereas elevated hydrostatic pressure results in a circular vesicle form of mitochondria (*arrowhead*) with abnormal cristae depletion (*arrow*) (**B**). The length of mitochondrial cross section was measured in control (mitochondria number, 222) and pressurized cells (mitochondria number, 217). *Significant at $P < 0.001$ compared with nonpressurized cells). (**C**) Data represent the mean ± SEM. Scale bar, 250 nm.

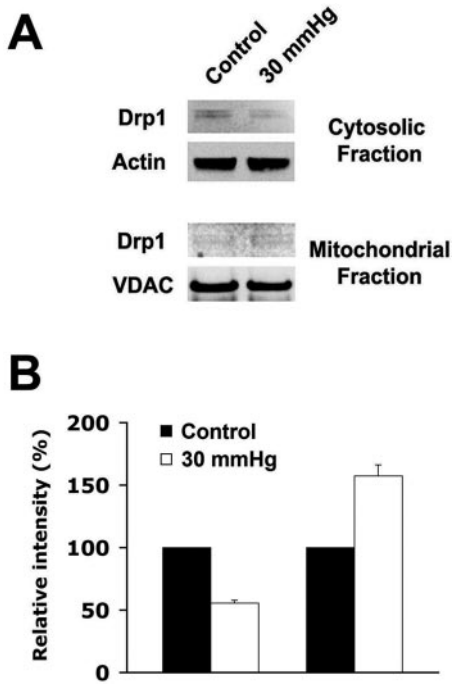

FIGURE 3. Pressure-induced translocation of Drp-1 from cytosol to mitochondria. After exposure to 30 mm Hg for 3 days, mitochondria were separated from cytosol by differential centrifugation, and Drp1 content was analyzed by Western blot analysis. (**A**) The Drp-1 protein bands show the positions, based on comparison with size standards, of the 80-kDa form of Drp-1. The blot was stripped and reprobed with anti-actin antibody (~42 kDa) for cytosol fraction and anti-VDAC antibody (~31 kDa) for mitochondrial fraction to confirm similar protein loading in each lane. (**B**) Relative intensity of chemiluminescence for each protein band was analyzed. Data represent the means ± SD of results in three independent experiments.

after elevated hydrostatic pressure. It has been reported that release of OPA1 during apoptosis participates in the rapid and complete release of cytochrome *c* and subsequent mitochondrial fragmentation.[40] In a separate study, we found that OPA1

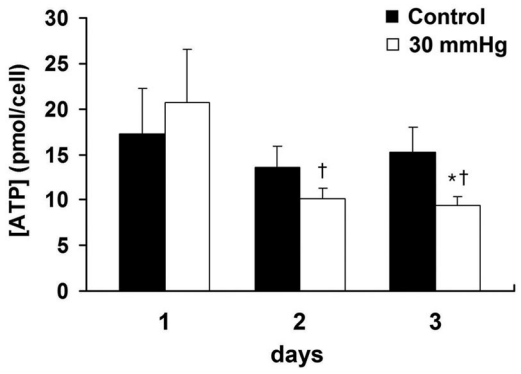

FIGURE 4. Cellular ATP reduction after exposure to elevated hydrostatic pressure. Differentiated RGC-5 cells plated in 96 wells in complete medium were exposed to elevated hydrostatic pressure (30 mm Hg) for 1, 2, or 3 days. ATP concentrations are shown as the mean ± SD normalized to the plating density of differentiated RGC-5 cells (n = 3; *Significant at $P < 0.05$ compared with nonpressurized cells at 3 days; †significant at $P < 0.05$ compared with pressurized cells at 1 day). There was no significance difference among nonpressurized cells at 1, 2, or 3 days. Data are representative of three or five independent experiments. Each data set is the mean ± SD of the signal obtained from 24 replicate wells.

translocates from mitochondria to the cytosol after elevated hydrostatic pressure (unpublished data). Together, the above findings show that elevated hydrostatic pressure induces mitochondrial fission and bioenergetic impairment in differentiated RGC-5 cells.

It has been suggested that increased ambient hydrostatic pressure of a defined incubation gas mix (5% CO_2 and air) on a liquid-phase culture medium could alter partial pressures of the vital gases O_2 and CO_2 and through alteration of dissolved CO_2 alter pH. If this had occurred, it could influence neuronal cell viability.[26] In our model, hydrostatic pressure did not cause any difference in pH or the vital gases in cultures subjected to pressure, compared with control cultures, suggesting that the pressure system did not significantly alter the gas relationships in the RGC-5 cultures. Our findings agree with studies using similar pressure chamber designs with other cell types showing a negligible impact on gas relationships within the culture medium.[26–28]

The RGC-5 cell line used for this investigation is a transformed retinal ganglion cell line that has certain characteristics of RGCs, including expression of Thy-1, Brn-3C, neuritin, NMDA receptor, GABA-B receptor, and synaptophysin.[24] These cells did not express glial fibrillary acidic protein, HPC-1, or 8A-1.[24] These similarities suggest that RGC-5 cells would respond to stresses such as pressure in a manner similar to primary RGCs in vivo. It has been reported that fluoresceinated sConA, a dimeric ConA derivative, localizes to Golgi and lysosomal structures and that cellular responses to sConA treatment include decreased growth rate, a reversible decrease in the phosphorylated state of a 41-kDa phosphoprotein, and

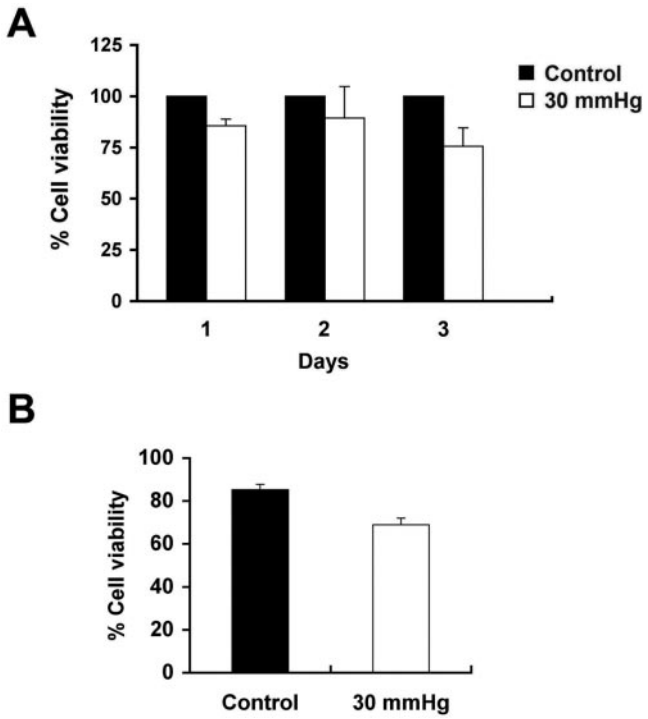

FIGURE 5. Cell viability after exposure to elevated hydrostatic pressure. Differentiated RGC-5 cells were treated with elevated pressure (30 mm Hg) for 1, 2, or 3 days. At each time point, cell viability in the control and experimental was measured by MTT assay (**A**). Data are presented as the percentage of cell viability in same-day control wells. Viability in cultures exposed to 30 mm Hg for 3 days was also assessed by trypan blue staining (**B**). Data are representative of results in three or five independent experiments. Each data set is the mean ± SD of the signal obtained from 24 replicate wells for MTT assay and from 5 replicate wells for trypan blue staining.

induction of neuron-specific enolase.[25] Further differentiation of RGC-5 cells occurs after their exposure to sConA, including slowed growth and the development of sensitivity to glutamate toxicity.[24] This is similar to the sConA-induced changes in LA29NR, a transformed neuroretinal cell line, including neurite outgrowth, increased cell-to-cell adhesion, and decreased growth rate.[25] However, several differences between LA29NR and differentiated RGC-5 cells and primary RGCs have been demonstrated, including their ability to proliferate, their non-neuronal appearance, and a lack of the repertoire of ion channels characteristic of primary RGCs.[24] Thus, differentiated RGC-5 cells appear to be a suitable model system for initial investigation of primary RGC responses to pressure. Further insight may be gained by repeating the present studies using purified primary RGC cultures, as well as by examining mitochondrial fission, cristae depletion and bioenergetic impairment in animal models of glaucoma.

The mechanism of pressure-induced cellular effects is not clear. One study has obtained evidence that pressure can induce conformational changes in aqueous humor proteins.[41] However, this finding is controversial.[42] In non-neuronal cells, pressure has been found to alter proliferation and morphologic changes in cultured bovine aortic endothelial cells, apoptotic cell death in neuronal cell lines (B35, PC12, C17, and NT2), and gene expression in human optic nerve astrocytes.[26,28,43] It is possible that pressure may alter the metabolic requirements of the RGC-5 cells. This alteration may contribute to earlier exhaustion of the energy sources in the pressure-treated cultures than in control cultures and should be explored in future studies. In addition to RGC-5 cells, recent evidence indicates that elevated hydrostatic pressure induces apoptotic death in primary cultures of purified RGCs.[29,44,45] Thus, further insight into the mechanism of this effect may be obtained by studying RGC mitochondria function in purified RGC cultures as well as in retinal slice cultures.

Mitochondria in the axons at the optic nerve head are highly concentrated in the unmyelinated regions proximal to the heminodes of Ranvier. The concentration of mitochondria suddenly decreases as the myelin sheath begins more posteriorly in the optic nerve, a specific site of damage in glaucoma.[46–49] Recent studies have suggested that mitochondrial distribution reflects the different energy requirements of the unmyelinated axons in comparison to the myelinated retrolaminar axons and that the unmyelinated portion of the optic nerve has greater demands for mitochondrially derived ATP than the myelinated posterior segment.[46,50] Thus, the present observation that increased pressure reduces mitochondrial ATP production suggests a local ATP deficit that may occur in the RGC axons of the glaucomatous optic nerve head. It has been reported that a deficiency in mitochondrially derived ATP causes RGC death in Leber's hereditary optic neuropathy.[51,52] Furthermore, a recent study has been demonstrated that mitochondrial fission is associated with reduced ATP production in cortical neuron exposed to *S*-nitrosocysteine (SNOC), a nitric oxide donor.[31] Although ATP reduction by itself is insufficient to identify the presence of bioenergetic alterations, our observation that ATP reduction was accompanied by cristae depletion does indicate that pressure treatment induced bioenergetic impairment in our model.[31] Thus, treatments that help mitochondria to recover from stress or that facilitate ATP production may help to protect the optic nerve in glaucoma.

In summary, we demonstrate that elevated hydrostatic pressure triggers mitochondrial fission and cellular ATP reduction in differentiated RGC-5 cells. Further investigation of the molecular mechanisms that regulate the cellular response to elevated pressure including mitochondrial fission may provide new therapeutic targets for protecting RGCs and the optic nerve from elevated pressure.

Acknowledgments

The authors thank Yulia E. Kushnareva (The Burnham Institute, San Diego, CA) and Ian A. Trounce (University of Melbourne) for helpful discussions.

References

1. Weinreb RN, Khaw PT. Primary open-angle glaucoma. *Lancet*. 2004;363:1711–1720.
2. Anderson DR, Hendrickson A. Effect of intraocular pressure on rapid axoplasmic transport in monkey optic nerve. *Invest Ophthalmol*. 1974;13:771–783.
3. Quigley HA, Addicks EM. Chronic experimental glaucoma in primates. II. Effect of extended intraocular pressure elevation on optic nerve head and axonal transport. *Invest Ophthalmol Vis Sci*. 1980;19:137–152.
4. Brenner C, Kroemer G. Apoptosis: mitochondria—the death signal integrators. *Science*. 2000;289:1150–1151.
5. Kroemer G, Reed JC. Mitochondrial control of cell death. *Nat Med*. 2000;6:513–519.
6. Chen H, Chan DC. Emerging functions of mammalian mitochondrial fusion and fission. *Hum Mol Genet*. 2005;14:R283–R2899.
7. Okamoto K, Shaw JM. Mitochondrial morphology and dynamics in yeast and multicellular eukaryotes. *Annu Rev Genet*. 2005;39:503–536.
8. Karbowski M, Youle RJ. Dynamics of mitochondrial morphology in healthy cells and during apoptosis. *Cell Death Differ*. 2003;10:870–880.
9. Nunnari J, Marshall WF, Straight A, Murray A, Sedat JW, Walter P. Mitochondrial transmission during mating in Saccharomyces cerevisiae is determined by mitochondrial fusion and fission and the intramitochondrial segregation of mitochondrial DNA. *Mol Biol Cell*. 1997;8:1233–1242.
10. Youle RJ, Karbowski M. Mitochondrial fission in apoptosis. *Nat Rev Mol Cell Biol*. 2005;6:657–663.
11. Lee YJ, Jeong SY, Karbowski M, Smith CL, Youle RJ. Roles of the mammalian mitochondrial fission and fusion mediators Fis1, Drp1, and Opa1 in apoptosis. *Mol Biol Cell*. 2004;15:5001–5011.
12. Karbowski M, Lee YJ, Gaume B, et al. Spatial and temporal association of Bax with mitochondrial fission sites, Drp1, and Mfn2 during apoptosis. *J Cell Biol*. 2002;159:931–938.
13. Frank S, Gaume B, Bergmann-Leitner ES, et al. The role of dynamin-related protein 1, a mediator of mitochondrial fission, in apoptosis. *Dev Cell*. 2001;1:515–525.
14. Desagher S, Martinou JC. Mitochondria as the central control point of apoptosis. *Trends Cell Biol*. 2000;10:369–377.
15. Tatton WG, Chalmers-Redman RM, Sud A, Podos SM, Mittag TW. Maintaining mitochondrial membrane impermeability. an opportunity for new therapy in glaucoma? *Surv Ophthalmol.* 2001;(suppl 3):S277–S283.
16. Charles I, Khalyfa A, Kumar DM, et al. Serum deprivation induces apoptotic cell death of transformed rat retinal ganglion cells via mitochondrial signaling pathways. *Invest Ophthalmol Vis Sci*. 2005;46:1330–1338.
17. Zhang Y, Cho CH, Atchaneeyasakul LO, McFarland T, Appukuttan B, Stout JT. Activation of the mitochondrial apoptotic pathway in a rat model of central retinal artery occlusion. *Invest Ophthalmol Vis Sci*. 2005;46:2133–2139.
18. Lieven CJ, Vrabec JP, Levin LA. The effects of oxidative stress on mitochondrial transmembrane potential in retinal ganglion cells. *Antioxid Redox Signal*. 2003;5:641–646.
19. Vrabec JP, Lieven CJ, Levin LA. Cell-type-specific opening of the retinal ganglion cell mitochondrial permeability transition pore. *Invest Ophthalmol Vis Sci*. 2003;44:2774–2782.
20. Mattson MP. Apoptosis in neurodegenerative disorders. *Nat Rev Mol Cell Biol*. 2000;1:120–129.
21. Wallace DC. Mitochondrial diseases in man and mouse. *Science*. 1999;283:1482–1488.
22. Mittag TW, Danias J, Pohorenec G, et al. Retinal damage after 3 to 4 months of elevated intraocular pressure in a rat glaucoma model. *Invest Ophthalmol Vis Sci*. 2000;41:3451–3459.

23. Abu-Amero KK, Morales J, Bosley TM. Mitochondrial abnormalities in patients with primary open-angle glaucoma. *Invest Ophthalmol Vis Sci*. 2006;47:2533–2542.
24. Krishnamoorthy RR, Agarwal P, Prasanna G, et al. Characterization of a transformed rat retinal ganglion cell line. *Brain Res Mol Brain Res*. 2001;86:1–12.
25. Seigel GM, Notter MF. Lectin-induced differentiation of transformed neuroretinal cells in vitro. *Exp Cell Res.* 199:240–247, 1992.
26. Sumpio BE, Widmann MD, Ricotta J, Awolesi MA, Watase M. Increased ambient pressure stimulates proliferation and morphologic changes in cultured endothelial cells. *J Cell Physiol.* 1994; 158:133–139.
27. Mattana J, Sankaran RT, Singhal PC. Increased applied pressure enhances the uptake of IgG complexes by macrophages. *Pathobiology*. 1996;64:40–45.
28. Agar A, Yip SS, Hill MA, Coroneo MT. Pressure related apoptosis in neuronal cell lines. *J Neurosci Res*. 2000;60:495–503.
29. Sappington RM, Chan M, Calkins DJ. Interleukin-6 protects retinal ganglion cells from pressure-induced death. *Invest Ophthalmol Vis Sci.* 2006;47:2932–2942.
30. Poot M, Zhang YZ, Kramer JA, et al. Analysis of mitochondrial morphology and function with novel fixable fluorescent stains. *J Histochem Cytochem.* 1996;44:1363–1372.
31. Barsoum MJ, Yuan H, Gerencser AA, et al. Nitric oxide induced mitochondrial fission is regulated by dynamin related GTPase in neurons. *EMBO J*. 2006;25:3900–3911.
32. Brorson JR, Schumacker PT, Zhang H. Nitric oxide acutely inhibits neuronal energy production. *J Neurosci*. 1999;19:147–158.
33. Yaffe MP. The machinery of mitochondrial inheritance and behavior. *Science*. 1999;283:1493–1497.
34. Bossy-Wetzel E, Barsoum MJ, Godzik A, Schwarzenbacher R, Lipton SA. Mitochondrial fission in apoptosis, neurodegeneration and aging. *Curr Opin Cell Biol*. 2003;15:706–716.
35. Olichon A, Baricault L, Gas N, et al. Loss of OPA1 perturbates the mitochondrial inner membrane structure and integrity, leading to cytochrome c release and apoptosis. *J Biol Chem*. 2003;278:7743–7746.
36. Hackenbrock CR. Ultrastructural bases for metabolically linked mechanical activity in mitochondria. I. Reversible ultrastructural changes with change in metabolic steady state in isolated liver mitochondria. *J Cell Biol*. 1966;30:269–297.
37. Perkins GA, Ellisman MH, Fox DA. Three-dimensional analysis of mouse rod and cone mitochondrial cristae architecture: bioenergetic and functional implications. *Mol Vis.* 2003;9:60–73.
38. Mannella CA. Structure and dynamics of the mitochondrial inner membrane cristae. *Biochim Biophys Acta.* 2006;1763:542–548.
39. Karbowski M, Arnoult D, Chen H, Chan DC, Smith CL, Youle RJ. Quantitation of mitochondrial dynamics by photolabeling of individual organelles shows that mitochondrial fusion is blocked during the Bax activation phase of apoptosis. *J Cell Biol*. 2004;164: 493–499.
40. Arnoult D, Rismanchi N, Grodet A, et al. Bax/Bal-dependent release of DDP/TIMM8a promotes Drp1-mediated mitochondrial fission and mitoptosis during programmed cell death. *Curr Biol*. 2005;15:2112–2118.
41. Knepper PA, Miller AM, Choi J, et al. Hypophosphorylation of aqueous humor sCD44 and primary open-angle glaucoma. *Invest Ophthalmol Vis Sci*. 2005;46:2829–2837.
42. Ethier CR, Johnson M. Hydrostatic pressure is not a surrogate for IOP in glaucoma (E-letter). *Invest Ophthalmol Vis Sci.* Available at http://www.iovs.org/cgi/eletters/46/8/2829#304. Published February 16, 2006.
43. Yang P, Agapova O, Parker A, et al. DNA microarray analysis of gene expression in human optic nerve head astrocytes in response to hydrostatic pressure. *Physiol Genomics*. 2004;17:157–169.
44. Tezel G, Wax MB. The mechanisms of hsp27 antibody-mediated apoptosis in retinal neuronal cells. *J Neurosci.* 2000;20:3552–3562.
45. Agar A, Li S, Agarwal N, Coroneo MT, Hill MA. Retinal ganglion cell line apoptosis induced by hydrostatic pressure. *Brain Res*. 2006; 1086:191–200.
46. Andrews RM, Griffiths PG, Johnson MA, Turnbull DM. Histochemical localisation of mitochondrial enzyme activity in human optic nerve and retina. *Br J Ophthalmol*. 1999;83:231–235.
47. Bristow EA, Griffiths PG, Andrews RM, Johnson MA, Turnbull DM. The distribution of mitochondrial activity in relation to optic nerve structure. *Arch Ophthalmol*. 2002;120:791–796.
48. Barron MJ, Griffiths P, Turnbull DM, Bates D, Nichols P. The distributions of mitochondria and sodium channels reflect the specific energy requirements and conduction properties of the human optic nerve head. *Br J Ophthalmol*. 2004;88:286–290.
49. Carelli V, Ross-Cisneros FN, Sadun AA. Mitochondrial dysfunction as a cause of optic neuropathies. *Prog Retin Eye Res*. 2004;23:53–89.
50. Yu Wai Man CY, Chinnery PF, Griffiths PG. Optic neuropathies–importance of spatial distribution of mitochondria as well as function. *Med Hypotheses*. 2005;65:1038–1042.
51. Brown MD, Voljavec AS, Lott MT, MacDonald I, Wallace DC. Leber's hereditary optic neuropathy: a model for mitochondrial neurodegenerative diseases. *FASEB J*. 1992;6:2791–2799.
52. Rizzo JF III. Adenosine triphosphate deficiency: a genre of optic neuropathy. *Neurology*. 1995;45:11–16.